Effects of a high fat diet on brain metabolism in rats: An in vivo ^{1}H-MRS study

By

Kayla Danielle Raider

Submitted to the graduate degree program in Molecular and Integrative Physiology and the Graduate Faculty of the University of Kansas in partial fulfillment of the requirements for the degree of Master of Science.

_____

Chairperson William Brooks, PhD

_____

Co-Chairperson John Stanford, PhD

_____

Janna Harris, PhD

Date Defended: September 3, 2014

The Thesis Committee for Kayla Danielle Raider
certifies that this is the approved version of the following thesis:

Effects of a high fat diet on brain metabolism in rats: An in vivo ^{1}H-MRS study

_____

Chairperson: William Brooks, PhD

_____

Co-Chairperson: John Stanford, PhD

Date approved: September 3, 2014

Abstract

Diet-induced obesity and its metabolic consequences can lead to neurological dysfunction and increase the risk of developing Alzheimer's disease (AD) and Parkinson's disease (PD). Despite these realities, the effects of a high fat diet on the central nervous system are not well understood. To better understand effects of high fat consumption on the metabolic status of brain regions affected by AD and PD, we used magnetic resonance spectroscopy (^{1}H-MRS) to measure neurochemicals in the hippocampus and in the striatum of rats fed a high-fat diet vs rats fed normal low-fat chow. We detected lower levels of total creatine (tCr: phosphocreatine; PCr + creatine; Cr) and higher glutamine in both the hippocampus and striatum of high fat-fed rats. Additional effects observed in the hippocampus included higher n-acetylaspartylglutamic acid (NAAG), and lower myo-inositol (Ins), *gamma*-Aminobutyric acid (GABA), and serine (Ser). Post-mortem tissue analyses revealed lower phosphorylated AMP-activated protein kinase (AMPK) and nuclear respiratory factor-1 (NRF-1) protein levels in the striatum but not the hippocampus. Overall, these changes indicate diet induced alterations in bioenergetic function and neurotransmission within both the hippocampal and striatal tissue.

Acknowledgements

I am using this opportunity to thank my mentors, Dr. William Brooks and Dr. John Stanford for their support throughout this process. I would also like to express my warm thanks to my committee members, Dr. Russell Swerdlow, Dr. Beth Levant, and Dr. In-Young Choi, as well as Dr. Janna Harris for providing encouraging support and advice. I am also sincerely grateful for the assistance of the lab mates who assisted in completing this study.

Thank you,

Kayla Raider

This study was supported by Hoglund Brain Imaging Center and NIH grants (P30 HD02528 to the Kansas Intellectual and Developmental Disabilities Research Center; P30 AGO35982 to the University of Kansas Alzheimer's Disease Center; RR0116745). Hoglund Brain Imaging Center is supported by a generous gift from Forrest and Sally Hoglund.

Table of Contents

Introduction

A high fat diet is strongly associated with increased oxidative stress, chronic neuroinflammation, altered mitochondrial function, and decreased hippocampal neurogenesis and plasticity. Thus, it has been suggested that diet-induced obesity may accelerate age-related pathologies and diseases, as well as heighten the brain's vulnerability to brain insults, which contribute significantly to cognitive decline and dementia (Bruce-Keller et al 2009, Uranga et al 2010). For example, retrospective studies have found that midlife obesity was associated with a 74% higher chance of developing dementia, while an elevation in BMI of only a single unit was associated with a 36% increase in AD. Conversely, those with low fat diets had significantly lower risk for AD (Bruce-Keller et al 2009, Whitmer et al 2005). The development of metabolic syndrome alone has been demonstrated to increase the risk of AD, while type II diabetes has been correlated with AD, increasing an individual's relative risk by 2-3 fold (Arvanitidis et al 2009, Leibson et al 1997). In an ex vivo proton nuclear magnetic resonance (^{1}H-NMR) study, 6-hydroxydopamine (6-OHDA)-lesioned rats modeling PD showed altered energy metabolism through changes in lactate, alanine, succinate, and Cr in the striatum(Gao et al 2013). These defects in energy metabolism have been implicated in various neurodegenerative diseases, and are potentially due to defects in mitochondrial ATP production (Sangar et al 2012) and alterations in cerebral perfusion and brain microvasculature. These alterations have also been shown to occur with obesity (Uranga et al 2010). Overall, there appears to be poorer metabolic buffering in CNS-related disorders including diabetes, AD and PD, which could be exacerbated by diet-induced obesity. Given the demographic projections of an older and more obese population, the public health consequences of these co-morbidities are dire. Despite this reality, the effects of a high fat diet on the central nervous system are not well understood.

We have conducted several studies examining the effects of a high fat diet on nigrostriatal function and vulnerability in young adult rats. We have reported that, like normal aging (Cass et al 2002, Marshall et al 1983), a high fat diet increases nigrostriatal dopamine (DA) depletion in the 6-OHDA rat model of PD (Morris et al 2010). We have also reported that unlesioned rats fed a high fat diet exhibit substantially attenuated striatal DA release and increased iron levels and markers of oxidative stress in the substantia nigra (Morris et al 2011). These findings also parallel findings reported for normal aging (Drayer et al 1986, Hebert & Gerhardt 1998, Ke et al 2005, Venkateshappa et al 2012a, Venkateshappa et al 2012b). Overall, these results support the hypothesis that a high fat diet produces significant adverse effects on neurological function. It is possible that disrupted brain energy metabolism plays a role in these effects.

Deriving primarily from glucose metabolism, the brain's high energy consumption makes it vulnerable to impaired energy production. Defects in glucose homeostasis, including hypo- and hyper-glycemia, adversely affect human brain health and cognitive function (Biessels et al 2006, Craft 2005). Diet-induced obesity can result in reduced cerebral glucose utilization, even where the majority of glucose utilization has not been shown to rely on insulin (Levin 1991). Insulin resistance, glucose transport abnormalities, and altered cerebral glucose metabolism are pathophysiological features associated with mitochondrial dysfunction that have been demonstrated to occur with AD. These events can appear up to decades prior to cognitive decline and pathological alterations (Businaro et al 2012, Chen & Zhong 2013), linking obesity with an increased risk of developing AD.

To better understand the effects of high fat consumption on the metabolic status of brain regions affected by AD and PD, we used magnetic resonance spectroscopy (^{1}H-MRS) to measure neurochemicals in the hippocampus and striatum of rats fed a high-fat diet vs rats fed normal low-fat chow. ^{1}H-MRS is a powerful and non-invasive brain imaging technique that our group has used to measure the effects of normal aging and traumatic brain injury on brain metabolic signatures (Harris et al 2012, Harris et al 2014). This technique is able to quantify up to 20 neurochemicals in a given region of interest (ROI). The goal of the current study was to generate similar metabolic signatures for the neural effects of a high fat diet. We also measured proteins related to bioenergetic function in hippocampal and striatal tissue collected post mortem.

Materials & Methods

Animals and diet.

Two month old male F344 rats were given access *ad libitum* to a high fat diet (60% calories from fat, n=6) or standard rat chow (4% calories from fat, n=6) for five months. This high fat feeding protocol is an established model of insulin resistance characterized by increased adiposity and hyperglycemia. Body weights were 374 ± 9 g and 420 ± 8 g for the chow and high fat groups respectively ($p<0.001$) on the day of imaging (Table 1).

Magnetic Resonance Imaging and Spectroscopy

Animals were fasted for 12 hours prior to the imaging procedure. Isoflurane was administered for 4 minutes at 4% prior to placing the animal in the magnet cradle where anesthesia was maintained at 1.5-3% during imaging. During imaging, respiration was monitored and body temperature was maintained at 37°C via a feedback control system. We collected water-suppressed STEAM spectra (Varian 9.4T spectrometer, TE=2ms, TR=4000ms) from two

ROI over the hippocampus and striatum (Figure 1). First and second order shims were adjusted using FASTMAP, and spectra (Figure 2) were analyzed with LCModel as described previously (Harris et al 2014).

Western Blot

Antibodies against NRF1, TFAM, phosph-AMPK, and total AMPK were obtained from Cell Signaling Technology (Beverly, MA), and antibodies against PGC1α were obtained from Calbiochem (San Diego, CA). Antibodies against Actin were obtained from Abcam (Cambridge, MA). Goat-anti-rabbit HRP-conjugated secondary antibodies were obtained from Santa Cruz Biotechnology (Santa Cruz, CA). Enhanced chemiluminescence reagents were purchased from Thermo Scientific (Waltham, MA). All other reagents were obtained from Sigma (St.Louis, MO).

Brains were extracted after MRS procedures were complete and tissue was dissected using a stainless steel adult rat brain slicer matrix with 1.0 mm coronal slice intervals. Sections of the hippocampus and striatum were dissected from the slices and frozen for later analysis.

Samples were processed for protein analysis as described previously (Morris et al 2008). Frozen samples were diluted in cell extraction buffer and the tissue was homogenized and centrifuged. A Bradford assay was performed in triplicate to determine sample protein concentrations and then diluted to obtain samples of constant concentration for analysis with SDS-PAGE. All samples were run on 10% gels and then transferred to nitrocellulose membranes, followed by blocking and incubation with primary and secondary antibodies for proper time intervals. Upon exposure, films were scanned at high resolution to obtain digital images. Densitometry analyses were performed using Image J software.

Statistical Analysis

For the MRS measurements, only those with Cramer-Rao lower bounds ≤ 30 were accepted. Neurochemical levels in the HF vs. control groups were compared using a weighted averages method, and corrected for multiple comparisons, as previously described *(Harris et al 2014)*.

Protein concentrations obtained with western immunoblot were compared between groups using an unpaired Student's t-test. Data are shown as the mean and standard error. For all analyses, statistical significance was set at $p \leq 0.05$.

Results

Neurochemical changes induced by a high fat diet in fasted animals.

Using ^{1}H-MRS, we evaluated 20 neurochemicals in two brain regions after 5 months of a high fat or standard chow diet (Table 2). These data showed that a long term high fat diet induces neurochemical changes in the striatum and hippocampus. Decreases in striatal (p=0.007) and hippocampal (p=0.007) tCr and increases in striatal (p=0.048) and hippocampal (p=0.010)gln were significant. The hippocampus showed changes in GABA (p=0.046), NAAG (p=0.003), Ins (p=0.003), and Ser (p=0.001) levels with the high fat diet as well. These neurochemicals were not affected in the striatum.

Protein effects of long term high fat diet.

We measured levels of three mitochondrial proteins and activation of AMPK in the striatum and hippocampus of fasted animals using western immunoblot (Figure A1). There was evidence of lower AMPK phosphorylation and NRF1 expression in the striatum of the high fat

fed animals (Fig. 3a, p=0.047, 0.025), while there were no significant diet effects in the hippocampus (Fig. 3b). While the effect did not reach statistical significance, PGC1α levels were lower in the striatal tissue (Fig. 3a, p=0.065) further suggesting mitochondrial alterations induced by the high fat diet.

Correlation between tCr and AMPK activation.

In order to determine relationships between imaging and tissue findings, we conducted correlation analyses (Table A1 of Appendix A). These analyses revealed a strong positive correlation between tCr levels and AMPK activation (r =0.708; p=0.000) Animals with lower tCr also had lower pAMPK/AMPK (Figure 4). This effect was strongest in the hippocampus (r=0.738; p=0.009; Figure 5).

Table 1 – Weight changes in control and high fat fed groups.

	Starting Weight (g)	Ending Weight (g)	Weight Gain (g)	%Weight Gain
Control	265 ± 3	374 ± 9	109 ± 10	41.1
High Fat	266 ± 4	420 ± 8	154 ± 9	57.9
p value	0.44	**0.0009**	**0.0007**	

Values are group means with standard error. $p < 0.05$ is denoted in bold.

Figure 1 - Sample voxels chosen for H-MRS. Regions of interest for hippocampus (left) and striatum (right) as identified on anatomical MRI taken from the coronal (top) and sagittal (bottom) planes.

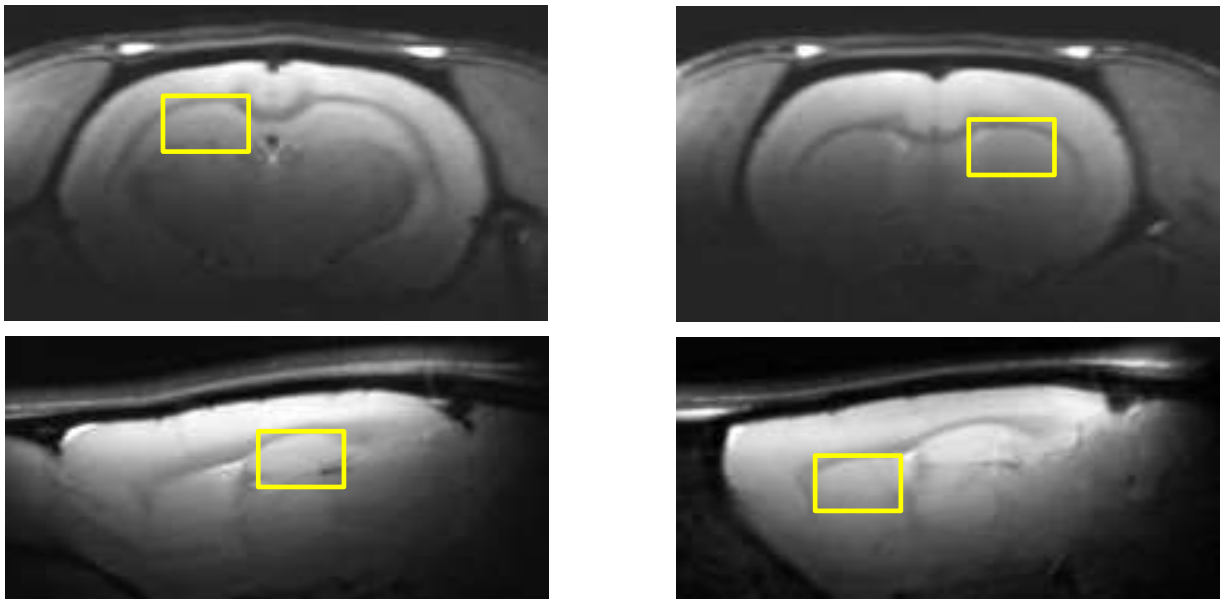

Figure 2 - Sample H-MRS Spectra

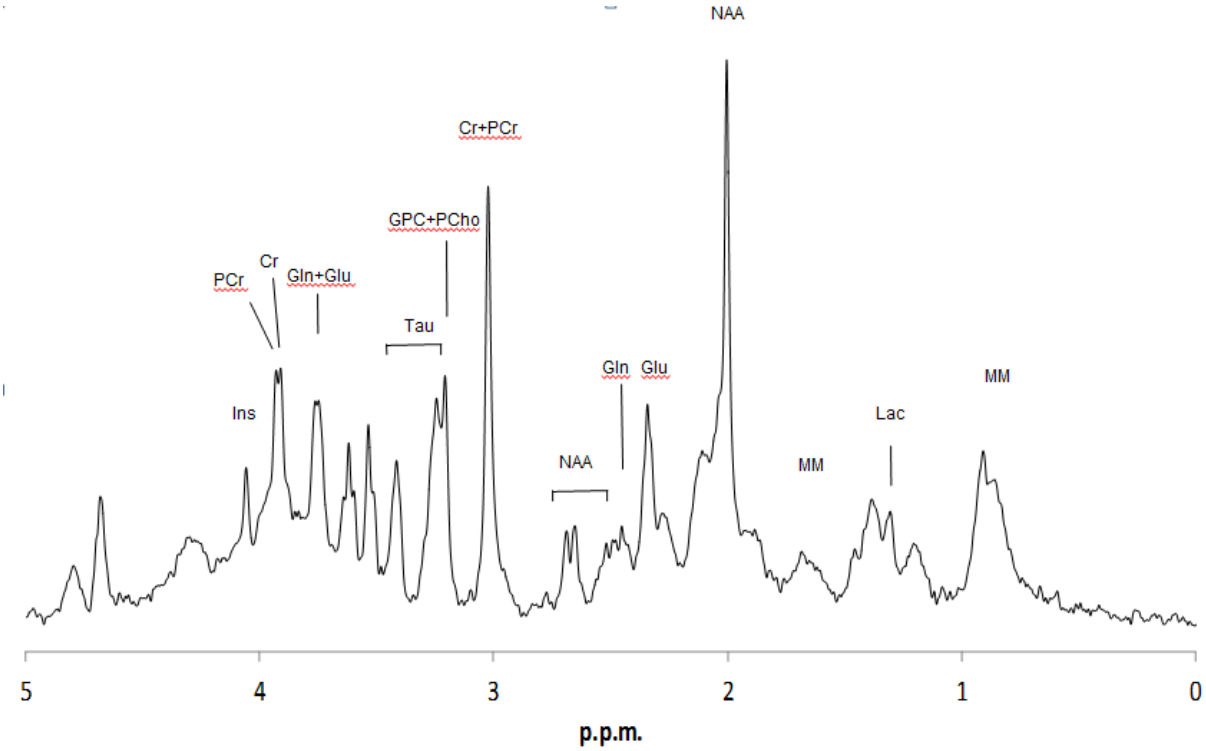

Table 2 – Neurochemical changes in the high fat fed vs. control animals.

	Hippocampus			**Striatum**		
	Control	High Fat	*p*	Control	High Fat	*P*
Ala	0.39 ± 0.04	0.38 ± 0.04	0.804	0.58 ± 0.05	0.45 ± 0.07	0.159
Asc	2.84 ± 0.26	2.33 ± 0.09	0.078	2.28 ± 0.16	2.13 ± 0.10	0.423
Asp	1.54 ± 0.23	1.31 ± 0.16	0.415	0.81 ± 0.15	0.83 ± 0.14	0.929
Cr	3.79 ± 0.11	3.28 ± 0.18	0.050	3.72 ± 0.21	3.42 ± 0.20	0.319
PCr	5.95 ± 0.24	5.58 ± 0.15	0.221	5.48 ± 0.28	5.34 ± 0.17	0.686
tCr	9.70 ± 0.22	8.77 ± 0.17	**0.007**	9.28 ± 0.17	8.80 ± 0.12	**0.038**
GABA	1.38 ± 0.06	1.20 ± 0.05	**0.046**	1.43 ± 0.10	1.33 ± 0.05	0.393
Glc	3.75 ± 0.57	3.34 ± 0.22	0.497	4.34 ± 0.49	5.09 ± 0.18	0.177
Gln	3.29 ± 0.12	3.71 ± 0.13	**0.048**	4.14 ± 0.12	4.62 ± 0.10	**0.010**
Glu	10.12 ± 0.05	9.59 ± 0.21	0.055	9.02 ± 0.15	9.06 ± 0.11	0.821
GPC	0.94 ± 0.07	0.81 ± 0.07	0.216	0.90 ± 0.04	0.81 ± 0.09	0.396
PCho	0.24 ± 0.04	0.22 ± 0.03	0.797	0.57 ± 0.04	0.55 ± 0.05	0.746
tCho	1.19 ± 0.08	1.04 ± 0.07	0.169	1.46 ± 0.03	1.37 ± 0.07	0.300
GSH	0.90 ± 0.07	0.85 ± 0.05	0.604	0.99 ± 0.03	0.98 ± 0.02	0.801
Ins	8.39 ± 0.21	7.35 ± 0.16	**0.003**	6.770 ± 0.13	6.49 ± 0.14	0.187
Lac	1.53 ± 0.07	1.63 ± 0.12	0.499	2.42 ± 0.35	1.78 ± 0.13	0.111
NAA	9.75 ± 0.11	9.72 ± 0.15	0.884	8.09 ± 0.26	8.36 ± 0.13	0.377
NAAG	0.82 ± 0.04	1.04 ± 0.04	**0.003**	0.98 ± 0.11	0.93 ± 0.04	0.656
PE	1.54 ± 0.41	1.58 ± 0.05	0.928	1.93 ± 0.19	1.85 ± 0.17	0.785
Ser	1.73 ± 0.18	0.82 ± 0.08	**0.001**	1.92 ± 0.22	1.73 ± 0.29	0.614
Tau	6.58 ± 0.19	6.38 ± 0.12	0.382	7.60 ± 0.21	7.52 ± 0.17	0.772
PCr/Cr	1.58 ± 0.14	1.72 ± 0.15	0.505	1.50 ± 0.14	1.56 ± 0.09	0.734

Neurochemical concentrations are expressed as mmol/g wet tissue weight. Values are weighted group means and weighted standard error. $p < 0.05$ is denoted in bold. Key: Ala, alanine; Asc, ascorbate, Asp, aspartate; Cr, creatine; GABA, gamma aminobutyric acid; Glc, glucose; Gln, glutamine; Glu, glutamate; GPC, glycerophosphocholine; GSH, glutathione; Ins, myo-inositol; Lac, lactate; NAA, N-acetylaspartate; NAAG, N-acetylaspartyl glutamate; PCho, phosphocholine; PCr, phosphocreatine; PE, phosphoethanolamine; Ser, serine; Tau, taurine; tCho, total choline (GPC & PCho); tCr, total creatine (Cr & PCr).

Figure 3 - Western immunoblot quantification of proteins in (a) striatal and (b) hippocampal tissue.

3a. Striatum

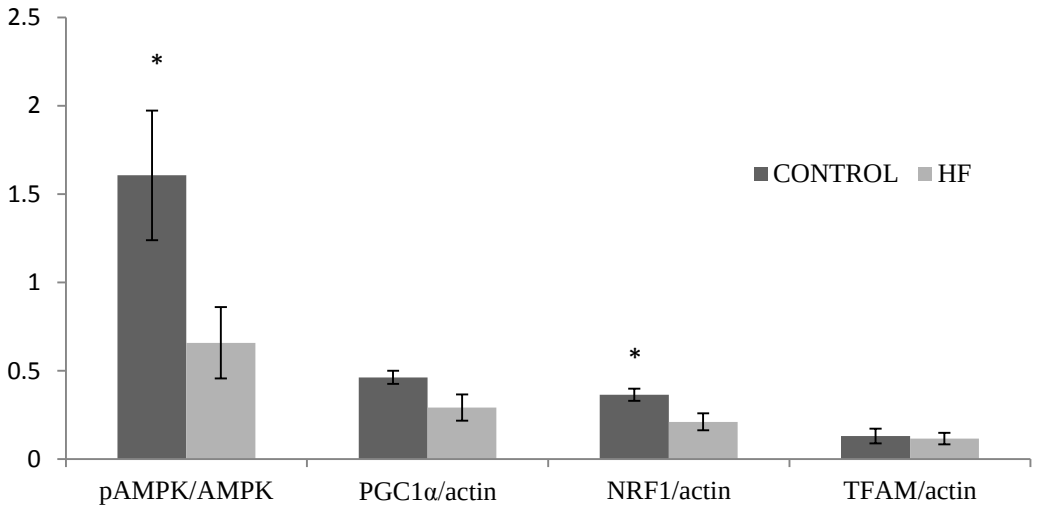

TFAM, *p*= 0.774; NRF1, *p*= 0.025; PGC1α, *p*= 0.065; pAMPK/AMPK, *p*= 0.047

3b. Hippocampus

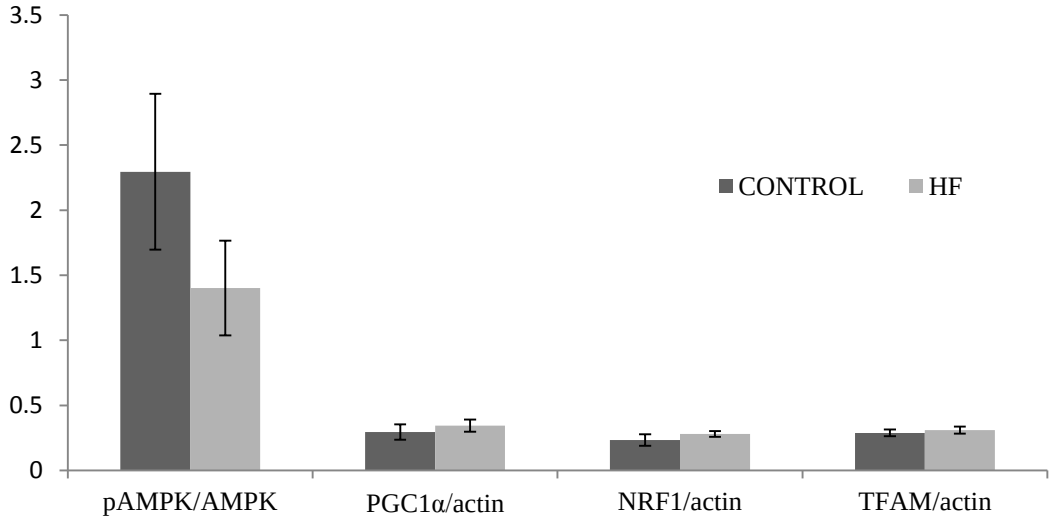

TFAM, *p*= 0.593; NRF1, *p*= 0.397; PGC1α, *p*= 0.542; pAMPK/AMPK, *p*= 0.258

Figure 4 - Total Creatine vs. Activation of AMPK in Brains of Fasted Rats

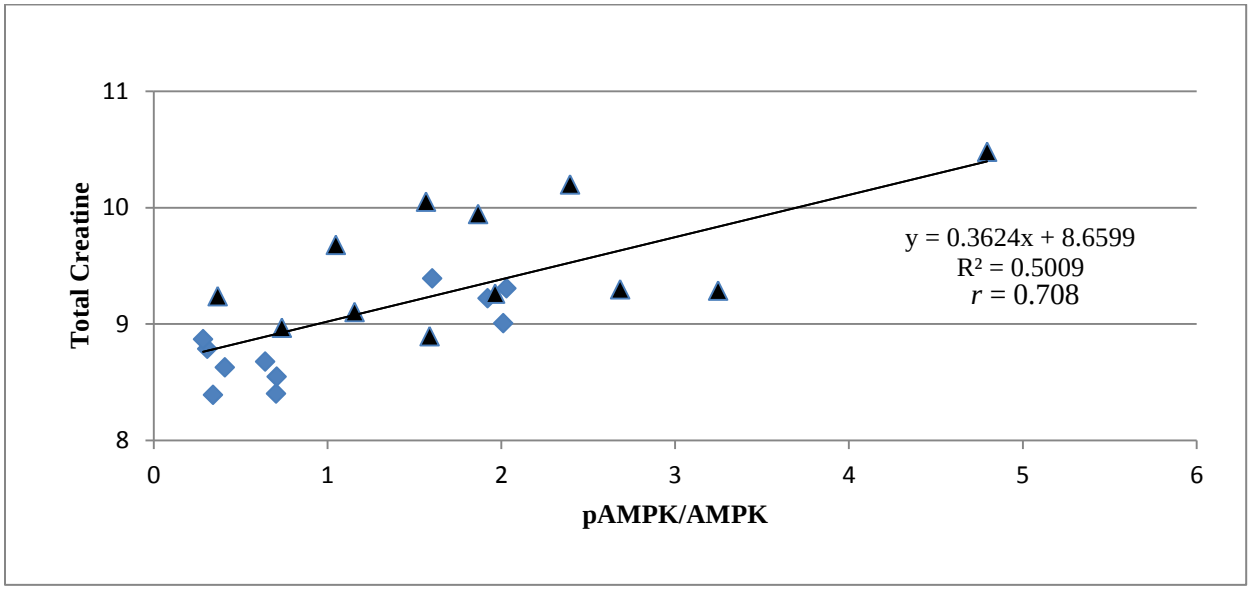

Measurements from control animals are indicated by triangle data points, and high fat fed animals by diamond data points. The correlation coefficient, *r*, is given and indicates a strong correlation between levels of total creatine and AMPK activation. This data is also shown for striatum and hippocampus tissue samples separately in Figures 5a and 5b.

Figure 5 – Total Creatine vs. Activation of AMPK in Striatum and Hippocampus

5a. Striatum

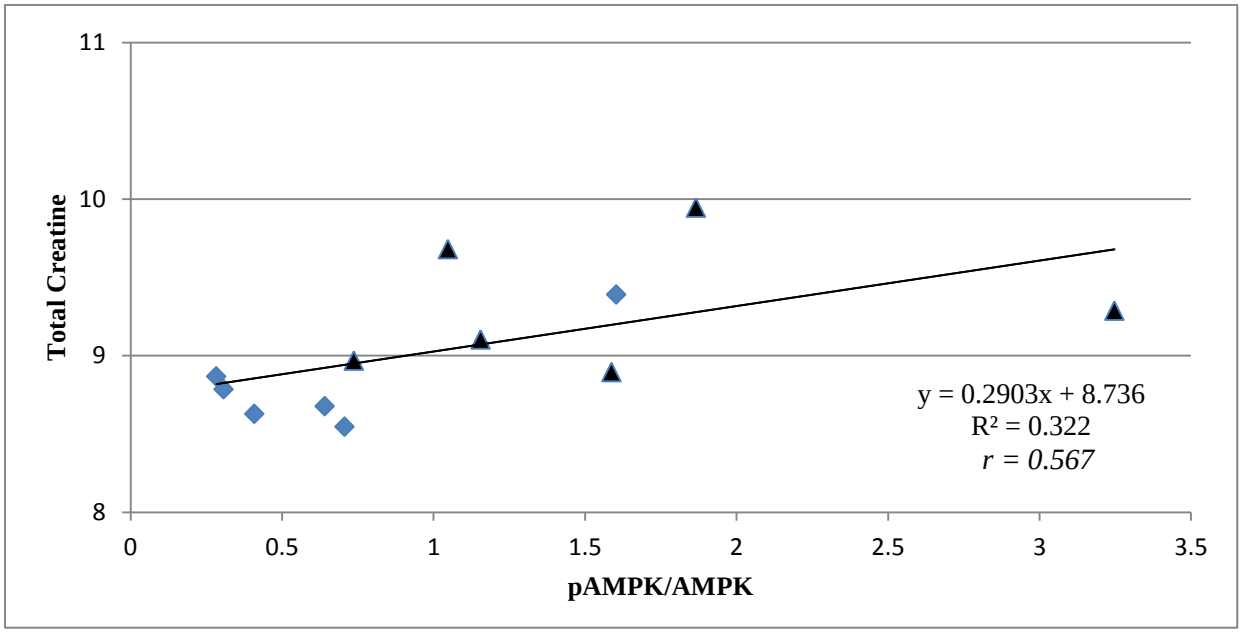

5b. Hippocampus

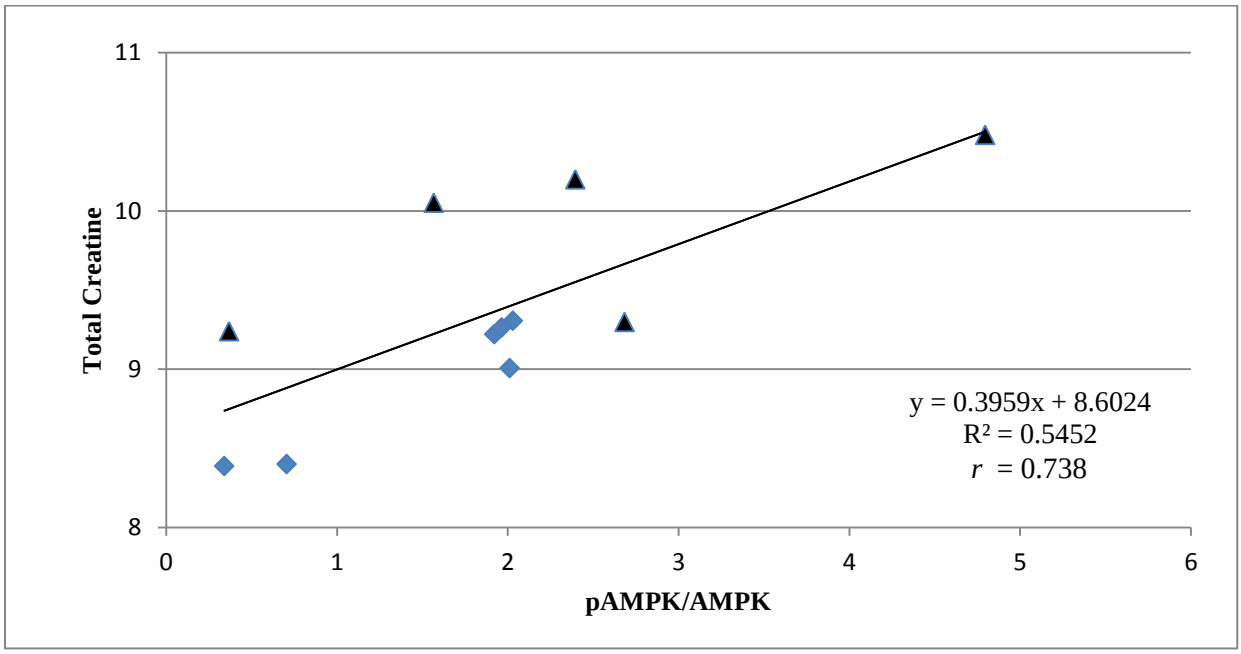

Discussion

This study reveals bioenergetic and metabolic neuronal changes induced by a high fat diet. While we did not observe evidence of significant oxidative stress or chronic inflammation known to be associated with the high fat diet, we did detect changes suggesting disrupted energy homeostasis and altered neurotransmission in both the hippocampus and striatum. The results of this study can assist in identifying mechanisms for how a high fat diet affects these brain tissues early on, and help elucidate the link between a diet high in fat and the development of neurodegenerative disease.

Decreases in total creatine & AMPK activation

Creatine (Cr) and phosphocreatine (PCr) are known to play a central role in energy metabolism, buffering against rapid changes in ADP/ATP ratios (Choe et al 2013). At times of high energy demand, PCr can be used to fuel metabolic needs, resulting in a decreased PCr:Cr ratio. Conversely, PCr can be reserved during times of low energy demand, resulting in higher PCr:Cr ratios providing an energy supply buffer, and signaling other pathways that are involved in energy regulation and homeostasis. While the individual values of Cr and PCr did not differ significantly between groups, Cr levels accounted for more of the reduction in tCr than pCr. Given this, we should have measured greater PCr:Cr ratios in the HF-fed animals. However, PCr:Cr ratios were similar between groups (Table 2). Alterations in the Cr-PCr system should result in diminished capacity to buffer energy needs and to activate further signaling cascades involved in metabolic regulation. Because PCr:Cr ratios did not differ between groups, we are unsure if the changes in Cr were related to the lower activation of AMPK in the high fat-fed animals. We did measure a strong correlation between tCr levels and AMPK activation (Figure

4). In general, it appears that the high fat-fed animals have lower tCr and lower AMPK activation in both brain regions. The immunoblot data did not show a significant difference in AMPK activation in the hippocampus, yet this is where the strongest correlation between Cr and AMPK was measured (Figure 5). Together, these data suggest that lower levels of tCr can potentially impact downstream events such as the activation of AMPK, even if PCr:Cr ratios are unchanged. One study reported that Cr deficiency actually induces chronic Cr-dependent activation of AMPK, stimulating catabolic pathways and providing protection against diet induced obesity (Choe et al 2013).

Because Cr levels are generally assumed to remain relatively constant, they are often used as an internal reference. However, under certain physiological conditions, such as hyperglycemia, this does not hold true (Karczewska-Kupczewska et al 2013). The lower Cr found in our study could potentially be due to reduced levels of Cr precursors or synthesis-related enzymes such as arginine:glycine amidinotransferase (AGAT). AGAT activity is regulated by growth hormone and thyroxine, both of which have been shown to be affected by high fat diets, obesity, and diabetes (List et al 2009, Lu et al 2013). Reduced Cr kinase activity was shown to be associated with HFD-induced metabolic changes (Amin et al 2011) and has been measured in the brains of streptozotocin- induced diabetic rats (Zhao et al 1999). It is possible that this effect is due to increased ROS production under these conditions (Genet et al 2000). Reduced Cr kinase activity should create a less efficient Cr-PCr system and likely affects total Cr levels.

AMPK is a protein coupled to whole body and cellular energy status, and is a major regulator of energy metabolism. AMPK is sensitive to cellular AMP/ATP ratios and becomes

activated via AMP binding and phosphorylation at its Thr172 residue by upstream kinases at times of metabolic stresses (Amato & Man 2011). Elevated energy demand also decreases the PCr:Cr ratio, which also plays a role in Cr-dependent AMPK activity(Choe et al 2013). Neurons are the most metabolically demanding cells. Because energy demand is coupled to glucose uptake, it has been suggested that AMPK plays a role in the glucose transport system in the brain (Amato & Man 2011).

Here, we found that a high fat diet was associated with lower phosphorylation of AMPK. This suggests either lower cellular energy demand, or less than optimal responses to energy demand by the cell. Reduction in AMPK activation is associated with obesity and plays a role in neurodegenerative diseases such as AD (Amato & Man 2011). Additionally, studies have shown that treatments providing chronic activation of AMPK can protect against diet-induced obesity, creating a potential treatment for obesity or T2D (Amato & Man 2011, Kahn et al 2005, Sarnowska et al 2013, Sung et al 2014, Woo et al 2014). Under normal (non-obese) conditions, increased leptin would accompany increased fat, followed by an increase in fatty acid oxidation via activation of AMPK (Yang & Barouch 2007). Leptin resistance is associated with obesity however, which may explain the reduced activation of AMPK that we observed, and may portend less oxidation of fatty acids. Overall, animals in the high fat group exhibited signs of diminished buffering capacity for energy metabolism, and poorer control of the signaling cascades which regulate cellular energy metabolism.

Increases in glutamine.

After glutamate (Glu) release, Gln is rapidly synthesized by glutamine synthase to allow for rapid Glu clearance as part of the Glu-Gln cycle. Because of this rapid process, changes in

Gln levels likely reflect Glu neurotransmission. The changes in Gln with high fat consumption which were seen here could be evidence of low grade chronic excitotoxicity, resulting in neuronal damage or cell death within these tissues. Obesity has been shown to impair synaptic transmission (Sickmann et al 2010, Valladolid-Acebes et al 2012), potentially due to changes in myelination (Bruce-Keller et al 2009). This increase in Gln could be explained by increases in glutamine synthase activity or upregulation of other mechanisms involved in Glu clearance which have been found in studies of diet-induced obesity (Langley & York 1990, Valladolid-Acebes et al 2012). It was suggested that these mechanisms result from excessive glucocorticoid activity and desensitized NMDA receptors. Obesity-associated leptin deficiency has also been shown to increase hypothalamic cerebral activation, indicating higher neuronal oxidative metabolism and Glu neurotransmission (Delgado et al 2011). Various studies have also shown obesity to be linked to altered Glu-Gln cycling; however, the direction of obesity-induced changes is inconsistent across studies (Langley & York 1990, Sickmann et al 2010, Sookoian & Pirola 2012, Valladolid-Acebes et al 2012).

As mentioned previously, obesity can affect brain glucose metabolism and energy homeostasis. Gln could play a role in these processes. As a product of the TCA cycle, we would expect increases in Gln if the TCA cycle is not functioning efficiently due to reduced TCA cycle enzymatic activity or mitochondrial dysfunction. Reduced brain glucose metabolism has been reported in models of obesity and type II diabetes, with a larger reduction in glucose metabolism via the TCA cycle than through glycolysis (Sickmann et al 2010). Similar alterations in neurotransmission and cerebral energy metabolism have been associated with aging (Harris et al 2014) and neurodegenerative diseases such as AD (Chen & Zhong 2013, Uranga et al 2010).

Decreased NRF1 expression

NRF1 is a mitochondrial protein responsible for mDNA transcription and replication as well as aerobic respiration (Uranga et al 2010). Several studies have reported links between diet-induced metabolic disturbances and mitochondrial alterations. For example, high fat diets have been shown to negatively affect the generation of energy in mitochondria, likely due to decreases in complex I activity (Nisoli et al 2007, Uranga et al 2010). Decreased expression of genes involved in mitochondrial biogenesis have also been observed (Bruce-Keller et al 2009, Sangar et al 2012, Uranga et al 2010). Altered biogenesis and efficiency of the mitochondrial machinery would be expected to compromise energy availability in the brain.

The mitochondrial changes reflected by lower NRF1 expression could also play a role in dysfunctional energy metabolism in the striatum, as suggested by the observed changes in tCr and pAMPK. Whether these changes occurred concomitantly, or one as the result of the other, we believe they reflect early changes in the metabolic machinery in the striatum. Although the effect did not reach significance, the lower levels of PGC1α in the striatum of the high fat-fed rats provide further evidence for mitochondrial alterations in this tissue.

Additional changes in hippocampal neurochemicals.

While the striatum showed evidence of alterations in protein expression, the hippocampus had greater neurochemical changes detected via MRS. Lower levels of Ser, GABA, and Ins along with higher levels of NAAG indicate further alterations in brain metabolism in this brain region.

Ser binds to NMDA receptors acting as a co-agonist and modulator of neurotransmission and neurotoxicity at glutamatergic synapses (Mohd Zain et al 2012, Radzishevsky et al 2013, Wolosker et al 2008), while GABA functions as the main inhibitory neurotransmitter in the CNS. The lower levels of striatal Ser and GABA shown here further suggest obesity-induced disruption of neurotransmission and could potentially lead to excitotoxicity. Additionally, we saw increases in striatal NAAG, a peptide neurotransmitter which binds to NMDA receptors (Bergeron & Coyle 2012, Bergeron et al 2004). It is likely that the increase in NAAG also plays a role in altered neurotransmission homeostasis alongside the changes in Gln, Ser and GABA.

Ins has been recognized as a glial cell marker, second messenger, osmoregulator and cell membrane constituent (Karczewska-Kupczewska et al 2013). Obesity and insulin resistance have been linked to early cerebral changes of Ins; however it was higher levels of Ins that were observed rather than the lower levels we measured in the hippocampus of our high fat-fed animals (Gonzales et al 2012, Haley et al 2010, Haley et al 2013, Karczewska-Kupczewska et al 2013). Higher levels of Ins are also associated with neurological disorders, including AD (Karczewska-Kupczewska et al 2013). There are also studies, however, that link increased levels of intracellular Gln with lower Ins (Shawcross et al 2004). These findings may indicate a buffering system in the context of cellular metabolic disturbances, and our findings may indicate a similar mechanism in the hippocampus of high fat-fed rats.

Summary

Our findings indicate that a long-term high fat diet in adult rats induces significant metabolic changes, suggesting bioenergetic dysfunction as well as alterations in

neurotransmission. With the presence of obesity and metabolic disorders on the rise, it is important to develop an understanding of these early diet-induced changes within the CNS in order to determine the link to cognitive decline and increased risk of neurological disorders. Our study provides evidence of changes that can be detected with a non-invasive neuroimaging technique that could be translated to human studies, furthering the potential for developing therapeutic options for cognitive impairment in individuals with metabolic disorders.

References

Amato S, Man HY. 2011. Bioenergy sensing in the brain: the role of AMP-activated protein kinase in neuronal metabolism, development and neurological diseases. *Cell cycle (Georgetown, Tex.)* 10: 3452-60

Amin KA, Kamel HH, Abd Eltawab MA. 2011. The relation of high fat diet, metabolic disturbances and brain oxidative dysfunction: modulation by hydroxy citric acid. *Lipids in health and disease* 10: 74

Arvanitidis AP, Corbett D, Colbourne F. 2009. A high fat diet does not exacerbate CA1 injury and cognitive deficits following global ischemia in rats. *Brain research* 1252: 192-200

Bergeron R, Coyle JT. 2012. NAAG, NMDA receptor and psychosis. *Current medicinal chemistry* 19: 1360-4

Bergeron R, Coyle JT, Tsai G, Greene RW. 2004. NAAG Reduces NMDA Receptor Current in CA1 Hippocampal Pyramidal Neurons of Acute Slices and Dissociated Neurons. *Neuropsychopharmacology* 30: 7-16

Biessels GJ, Koffeman A, Scheltens P. 2006. Diabetes and cognitive impairment. Clinical diagnosis and brain imaging in patients attending a memory clinic. *Journal of neurology* 253: 477-82

Bruce-Keller AJ, Keller JN, Morrison CD. 2009. Obesity and vulnerability of the CNS. *Biochimica et biophysica acta* 1792: 395-400

Businaro R, Ippoliti F, Ricci S, Canitano N, Fuso A. 2012. Alzheimer's disease promotion by obesity: induced mechanisms-molecular links and perspectives. *Current gerontology and geriatrics research* 2012: 986823

Cass WA, Harned ME, Bailey SL. 2002. Enhanced effects of 6-hydroxydopamine on evoked overflow of striatal dopamine in aged rats. *Brain research* 938: 29-37

Chen Z, Zhong C. 2013. Decoding Alzheimer's disease from perturbed cerebral glucose metabolism: implications for diagnostic and therapeutic strategies. *Progress in neurobiology* 108: 21-43

Choe CU, Nabuurs C, Stockebrand MC, Neu A, Nunes P, et al. 2013. L-arginine:glycine amidinotransferase deficiency protects from metabolic syndrome. *Human molecular genetics* 22: 110-23

Craft S. 2005. Insulin resistance and cognitive impairment: a view through the prism of epidemiology. *Archives of neurology* 62: 1043-4

Delgado TC, Violante IR, Nieto-Charques L, Cerdan S. 2011. Neuroglial metabolic compartmentation underlying leptin deficiency in the obese ob/ob mice as detected by magnetic resonance imaging and spectroscopy methods. *Journal of cerebral blood flow and metabolism : official journal of the International Society of Cerebral Blood Flow and Metabolism* 31: 2257-66

Drayer B, Burger P, Darwin R, Riederer S, Herfkens R, Johnson GA. 1986. MRI of brain iron. *AJR. American journal of roentgenology* 147: 103-10

Gao HC, Zhu H, Song CY, Lin L, Xiang Y, et al. 2013. Metabolic changes detected by ex vivo high resolution 1H NMR spectroscopy in the striatum of 6-OHDA-induced Parkinson's rat. *Molecular neurobiology* 47: 123-30

Genet S, Kale RK, Baquer NZ. 2000. Effects of free radicals on cytosolic creatine kinase activities and protection by antioxidant enzymes and sulfhydryl compounds. *Molecular and cellular biochemistry* 210: 23-8

Gonzales MM, Tarumi T, Eagan DE, Tanaka H, Vaghasia M, Haley AP. 2012. Indirect effects of elevated body mass index on memory performance through altered cerebral metabolite concentrations. *Psychosomatic medicine* 74: 691-8

Haley AP, Gonzales MM, Tarumi T, Miles SC, Goudarzi K, Tanaka H. 2010. Elevated cerebral glutamate and myo-inositol levels in cognitively normal middle-aged adults with metabolic syndrome. *Metabolic brain disease* 25: 397-405

Haley AP, Gonzales MM, Tarumi T, Tanaka H. 2013. Dyslipidemia links obesity to early cerebral neurochemical alterations. *Obesity (Silver Spring, Md.)* 21: 2007-13

Harris JL, Yeh HW, Choi IY, Lee P, Berman NE, et al. 2012. Altered neurochemical profile after traumatic brain injury: (1)H-MRS biomarkers of pathological mechanisms. *Journal of cerebral blood flow and metabolism : official journal of the International Society of Cerebral Blood Flow and Metabolism* 32: 2122-34

Harris JL, Yeh HW, Swerdlow RH, Choi IY, Lee P, Brooks WM. 2014. High-field proton magnetic resonance spectroscopy reveals metabolic effects of normal brain aging. *Neurobiology of aging* 35: 1686-94

Hebert MA, Gerhardt GA. 1998. Normal and drug-induced locomotor behavior in aging: comparison to evoked DA release and tissue content in fischer 344 rats. *Brain research* 797: 42-54

Kahn BB, Alquier T, Carling D, Hardie DG. 2005. AMP-activated protein kinase: ancient energy gauge provides clues to modern understanding of metabolism. *Cell metabolism* 1: 15-25

Karczewska-Kupczewska M, Tarasow E, Nikolajuk A, Stefanowicz M, Matulewicz N, et al. 2013. The effect of insulin infusion on the metabolites in cerebral tissues assessed with proton magnetic resonance spectroscopy in young healthy subjects with high and low insulin sensitivity. *Diabetes care* 36: 2787-93

Ke Y, Chang YZ, Duan XL, Du JR, Zhu L, et al. 2005. Age-dependent and iron-independent expression of two mRNA isoforms of divalent metal transporter 1 in rat brain. *Neurobiology of aging* 26: 739-48

Langley SC, York DA. 1990. Increased type II glucocorticoid-receptor numbers and glucocorticoid-sensitive enzyme activities in the brain of the obese Zucker rat. *Brain research* 533: 268-74

Leibson CL, Rocca WA, Hanson VA, Cha R, Kokmen E, et al. 1997. The risk of dementia among persons with diabetes mellitus: a population-based cohort study. *Annals of the New York Academy of Sciences* 826: 422-7

Levin BE. 1991. Defective cerebral glucose utilization in diet-induced obese rats. *The American journal of physiology* 261: R787-92

List EO, Palmer AJ, Berryman DE, Bower B, Kelder B, Kopchick JJ. 2009. Growth hormone improves body composition, fasting blood glucose, glucose tolerance and liver triacylglycerol in a mouse model of diet-induced obesity and type 2 diabetes. *Diabetologia* 52: 1647-55

Lu C, Kumar PA, Sun J, Aggarwal A, Fan Y, et al. 2013. Targeted deletion of growth hormone (GH) receptor in macrophage reveals novel osteopontin-mediated effects of GH on glucose homeostasis and insulin sensitivity in diet-induced obesity. *The Journal of biological chemistry* 288: 15725-35

Marshall JF, Drew MC, Neve KA. 1983. Recovery of function after mesotelencephalic dopaminergic injury in senescence. *Brain research* 259: 249-60

Mohd Zain Z, Ab Ghani S, O'Neill RD. 2012. Amperometric microbiosensor as an alternative tool for investigation of D-serine in brain. *Amino acids* 43: 1887-94

Morris JK, Bomhoff GL, Gorres BK, Davis VA, Kim J, et al. 2011. Insulin resistance impairs nigrostriatal dopamine function. *Experimental neurology* 231: 171-80

Morris JK, Bomhoff GL, Stanford JA, Geiger PC. 2010. Neurodegeneration in an animal model of Parkinson's disease is exacerbated by a high-fat diet. *American journal of physiology. Regulatory, integrative and comparative physiology* 299: R1082-90

Morris JK, Zhang H, Gupte AA, Bomhoff GL, Stanford JA, Geiger PC. 2008. Measures of striatal insulin resistance in a 6-hydroxydopamine model of Parkinson's disease. *Brain research* 1240: 185-95

Nisoli E, Clementi E, Carruba MO, Moncada S. 2007. Defective mitochondrial biogenesis: a hallmark of the high cardiovascular risk in the metabolic syndrome? *Circulation research* 100: 795-806

Radzishevsky I, Sason H, Wolosker H. 2013. D-serine: physiology and pathology. *Current opinion in clinical nutrition and metabolic care* 16: 72-5

Sangar V, Eddy JA, Simeonidis E, Price ND. 2012. Mechanistic modeling of aberrant energy metabolism in human disease. *Frontiers in physiology* 3: 404

Sarnowska E, Balcerak A, Olszyna-Serementa M, Kotlarek D, Sarnowski TJ, Siedlecki JA. 2013. [AMP-activated protein kinase (AMPK) as therapeutic target]. *Postepy higieny i medycyny doswiadczalnej (Online)* 67: 750-60

Shawcross DL, Balata S, Olde Damink SW, Hayes PC, Wardlaw J, et al. 2004. Low myo-inositol and high glutamine levels in brain are associated with neuropsychological deterioration after induced hyperammonemia. *American journal of physiology. Gastrointestinal and liver physiology* 287: G503-9

Sickmann HM, Waagepetersen HS, Schousboe A, Benie AJ, Bouman SD. 2010. Obesity and type 2 diabetes in rats are associated with altered brain glycogen and amino-acid homeostasis. *Journal of cerebral blood flow and metabolism : official journal of the International Society of Cerebral Blood Flow and Metabolism* 30: 1527-37

Sookoian S, Pirola CJ. 2012. Alanine and aspartate aminotransferase and glutamine-cycling pathway: their roles in pathogenesis of metabolic syndrome. *World journal of gastroenterology : WJG* 18: 3775-81

Sung YY, Kim DS, Kim HK. 2014. Viola mandshurica ethanolic extract prevents high-fat-diet-induced obesity in mice by activating AMP-activated protein kinase. *Environmental toxicology and pharmacology* 38: 41-50

Uranga RM, Bruce-Keller AJ, Morrison CD, Fernandez-Kim SO, Ebenezer PJ, et al. 2010. Intersection between metabolic dysfunction, high fat diet consumption, and brain aging. *Journal of neurochemistry* 114: 344-61

Valladolid-Acebes I, Merino B, Principato A, Fole A, Barbas C, et al. 2012. High-fat diets induce changes in hippocampal glutamate metabolism and neurotransmission. *American journal of physiology. Endocrinology and metabolism* 302: E396-402

Venkateshappa C, Harish G, Mahadevan A, Srinivas Bharath MM, Shankar SK. 2012a. Elevated oxidative stress and decreased antioxidant function in the human hippocampus and frontal cortex with increasing age: implications for neurodegeneration in Alzheimer's disease. *Neurochemical research* 37: 1601-14

Venkateshappa C, Harish G, Mythri RB, Mahadevan A, Bharath MM, Shankar SK. 2012b. Increased oxidative damage and decreased antioxidant function in aging human substantia nigra compared to striatum: implications for Parkinson's disease. *Neurochemical research* 37: 358-69

Whitmer RA, Gunderson EP, Barrett-Connor E, Quesenberry CP, Jr., Yaffe K. 2005. Obesity in middle age and future risk of dementia: a 27 year longitudinal population based study. *BMJ (Clinical research ed.)* 330: 1360

Wolosker H, Dumin E, Balan L, Foltyn VN. 2008. D-amino acids in the brain: D-serine in neurotransmission and neurodegeneration. *The FEBS journal* 275: 3514-26

Woo SL, Xu H, Li H, Zhao Y, Hu X, et al. 2014. Metformin ameliorates hepatic steatosis and inflammation without altering adipose phenotype in diet-induced obesity. *PloS one* 9: e91111

Yang R, Barouch LA. 2007. Leptin signaling and obesity: cardiovascular consequences. *Circulation research* 101: 545-59

Zhao X, Bassirat M, Zeinab K, Helme RD. 1999. Effects of diabetes on creatine kinase activity in streptozotocin-diabetic rats. *Chinese medical journal* 112: 1028-31

Appendix A

Table A1 – Correlation Matrix of all ^{1}H-MRS and Western Immunoblot Data

		pAMPK/AMPK	Cr+PCr	Mac	Ala	Asc	Asp	bHB	GPC
pAMPK/AMPK	*r*	1	.708**	0.213	-0.225	0.09	.658**	0.149	0.099
	p		0	0.329	0.302	0.683	0.001	0.497	0.653
Cr+PCr	*r*	.708**	1	-0.148	-0.19	0.357	.645**	0.126	0.388
	p	0		0.49	0.373	0.087	0.001	0.558	0.061
Mac	*r*	0.213	-0.148	1	-0.188	0.012	0.225	-0.368	-0.203
	p	0.329	0.49		0.379	0.957	0.29	0.077	0.342
Ala	*r*	-0.225	-0.19	-0.188	1	-0.262	-.548**	0.209	-.446*
	p	0.302	0.373	0.379		0.216	0.006	0.326	0.029
Asc	*r*	0.09	0.357	0.012	-0.262	1	.476*	-0.233	.667**
	p	0.683	0.087	0.957	0.216		0.019	0.274	0
Asp	*r*	.658**	.645**	0.225	-.548**	.476*	1	-0.057	0.364
	p	0.001	0.001	0.29	0.006	0.019		0.79	0.081
bHB	*r*	0.149	0.126	-0.368	0.209	-0.233	-0.057	1	-0.053
	p	0.497	0.558	0.077	0.326	0.274	0.79		0.804
GPC	*r*	0.099	0.388	-0.203	-.446*	.667**	0.364	-0.053	1
	p	0.653	0.061	0.342	0.029	0	0.081	0.804	
PCho	*r*	-0.365	-0.219	-.617**	.565**	-0.344	-.635**	0.253	-0.219
	p	0.086	0.304	0.001	0.004	0.1	0.001	0.233	0.304
Cr	*r*	0.168	.480*	-0.266	-0.198	0.365	0.192	-0.156	.527**
	p	0.443	0.018	0.209	0.355	0.079	0.369	0.466	0.008
PCr	*r*	.613**	.645**	0.074	-0.03	0.062	.519**	0.269	-0.047
	p	0.002	0.001	0.73	0.888	0.773	0.009	0.203	0.828
GABA	*r*	0.142	0.291	-.597**	0.118	0.089	0.042	0.206	0.18
	p	0.519	0.168	0.002	0.584	0.68	0.847	0.334	0.401
Glc	*r*	-.662**	-0.307	-.564**	0.355	0.106	-.460*	0.103	0.075
	p	0.001	0.144	0.004	0.088	0.623	0.024	0.633	0.729
Gln	*r*	-.415*	-0.266	-0.294	0.303	-.511*	-.444*	0.15	-0.232
	p	0.049	0.208	0.163	0.15	0.011	0.03	0.484	0.274
Glu	*r*	.447*	.556**	0.344	-0.392	.508*	.718**	-0.159	0.287
	p	0.032	0.005	0.1	0.058	0.011	0	0.458	0.174
GSH	*r*	-0.268	-0.057	-0.265	0.316	0.221	-0.279	-0.053	.449*
	p	0.216	0.793	0.211	0.133	0.3	0.187	0.806	0.028

		pAMPK/AMPK	Cr+PCr	Mac	Ala	Asc	Asp	bHB	GPC
Ins	*r*	.559**	.703**	0.311	-.448*	.650**	.807**	-0.097	.411*
	p	0.006	0	0.14	0.028	0.001	0	0.653	0.046
Lac	*r*	-0.054	-0.188	-0.021	0.358	-.458*	-.486*	0.342	-0.249
	p	0.807	0.38	0.922	0.086	0.024	0.016	0.102	0.241
NAA	*r*	.414*	0.391	.438*	-.530**	0.404	.703**	-0.331	0.091
	p	0.049	0.059	0.032	0.008	0.05	0	0.114	0.672
NAAG	*r*	-0.229	-.458*	-0.045	0.207	-0.387	-0.382	0.217	-.407*
	p	0.292	0.025	0.833	0.333	0.062	0.066	0.308	0.048
PE	*r*	0.398	0.169	-0.009	0.212	-.721**	0.013	0.333	-.479*
	p	0.06	0.429	0.965	0.32	0	0.953	0.112	0.018
Ser	*r*	-0.334	0.15	-.636**	0.021	0.367	-0.163	0.042	.607**
	p	0.119	0.484	0.001	0.924	0.078	0.445	0.846	0.002
Tau	*r*	0.067	0.221	-.410*	0.2	-.407*	-0.193	0.253	0.034
	p	0.76	0.3	0.047	0.348	0.048	0.366	0.233	0.874
NAA+ NAAG	*r*	0.376	0.297	.437*	-.494*	0.326	.632**	-0.289	0.002
	p	0.077	0.159	0.033	0.014	0.12	0.001	0.17	0.992
Glu+Gln	*r*	0	0.288	0.033	-0.075	-0.037	0.259	0	0.043
	p	1	0.173	0.877	0.729	0.864	0.222	1	0.844
GPC+ PCho	*r*	-0.255	0.094	-.680**	0.162	0.19	-0.282	0.179	.541**
	p	0.241	0.661	0	0.45	0.373	0.182	0.401	0.006
PGC1α	*r*	0.061	-0.108	-0.186	0.301	-0.145	-0.21	0.096	-0.362
	p	0.782	0.623	0.396	0.162	0.51	0.336	0.662	0.09
NRF1	*r*	0.19	-0.042	-0.111	0.372	-0.068	-0.106	0.212	-0.299
	p	0.386	0.848	0.615	0.08	0.759	0.631	0.332	0.166
TFAM	*r*	.431*	0.23	.544**	-0.18	0.297	.624**	-0.112	-0.033
	p	0.04	0.29	0.007	0.41	0.169	0.001	0.611	0.881

**. Correlation is significant at the 0.01 level (2-tailed).

*. Correlation is significant at the 0.05 level (2-tailed).

(*r*)Pearson Correlation

(*p*)2-Tailed Significance

Table A1 (continued)

		PCho	Cr	PCr	GABA	Glc	Gln	Glu	GSH
pAMPK/AMPK	*r*	-0.365	0.168	.613**	0.142	-.662**	-.415*	.447*	-0.268
	p	0.086	0.443	0.002	0.519	0.001	0.049	0.032	0.216
Cr+PCr	*r*	-0.219	.480*	.645**	0.291	-0.307	-0.266	.556**	-0.057
	p	0.304	0.018	0.001	0.168	0.144	0.208	0.005	0.793
Mac	*r*	-.617**	-0.266	0.074	-.597**	-.564**	-0.294	0.344	-0.265
	p	0.001	0.209	0.73	0.002	0.004	0.163	0.1	0.211
Ala	*r*	.565**	-0.198	-0.03	0.118	0.355	0.303	-0.392	0.316
	p	0.004	0.355	0.888	0.584	0.088	0.15	0.058	0.133
Asc	*r*	-0.344	0.365	0.062	0.089	0.106	-.511*	.508*	0.221
	p	0.1	0.079	0.773	0.68	0.623	0.011	0.011	0.3
Asp	*r*	-.635**	0.192	.519**	0.042	-.460*	-.444*	.718**	-0.279
	p	0.001	0.369	0.009	0.847	0.024	0.03	0	0.187
bHB	*r*	0.253	-0.156	0.269	0.206	0.103	0.15	-0.159	-0.053
	p	0.233	0.466	0.203	0.334	0.633	0.484	0.458	0.806
GPC	*r*	-0.219	.527**	-0.047	0.18	0.075	-0.232	0.287	.449*
	p	0.304	0.008	0.828	0.401	0.729	0.274	0.174	0.028
PCho	*r*	1	0.014	-0.245	0.257	.646**	.661**	-.569**	0.339
	p		0.949	0.249	0.225	0.001	0	0.004	0.105
Cr	*r*	0.014	1	-0.361	0.394	0.011	-0.111	0.038	0.274
	p	0.949		0.083	0.057	0.96	0.604	0.859	0.194
PCr	*r*	-0.245	-0.361	1	-0.034	-0.336	-0.186	.557**	-0.299
	p	0.249	0.083		0.874	0.108	0.384	0.005	0.156
GABA	*r*	0.257	0.394	-0.034	1	0.37	-0.068	-0.021	0.232
	p	0.225	0.057	0.874		0.075	0.753	0.922	0.275
Glc	*r*	.646**	0.011	-0.336	0.37	1	0.384	-0.353	.470*
	p	0.001	0.96	0.108	0.075		0.064	0.091	0.021
Gln	*r*	.661**	-0.111	-0.186	-0.068	0.384	1	-.576**	0.364
	p	0	0.604	0.384	0.753	0.064		0.003	0.08
Glu	*r*	-.569**	0.038	.557**	-0.021	-0.353	-.576**	1	-0.202
	p	0.004	0.859	0.005	0.922	0.091	0.003		0.343
GSH	*r*	0.339	0.274	-0.299	0.232	.470*	0.364	-0.202	1
	p	0.105	0.194	0.156	0.275	0.021	0.08	0.343	
Ins	*r*	-.632**	0.289	.496*	0.053	-0.335	-.653**	.842**	-0.254
	p	0.001	0.171	0.014	0.804	0.109	0.001	0	0.232
Lac	*r*	0.343	0.15	-0.33	0.056	-0.099	0.34	-.522**	0.117
	p	0.101	0.485	0.116	0.796	0.645	0.104	0.009	0.587

		PCho	Cr	PCr	GABA	Glc	Gln	Glu	GSH
NAA	*r*	-.742**	0.038	0.382	-0.083	-.467*	-.619**	.841**	-0.399
	p	0	0.859	0.066	0.701	0.021	0.001	0	0.054
NAAG	*r*	0.08	-0.138	-0.366	0.175	0.133	0.089	-.490*	-0.18
	p	0.709	0.52	0.078	0.413	0.536	0.679	0.015	0.399
PE	*r*	0.109	-0.15	0.31	0.074	-0.339	0.33	-0.326	-0.232
	p	0.613	0.484	0.14	0.73	0.105	0.115	0.12	0.276
Ser	*r*	.501*	.541**	-0.311	0.376	.620**	0.227	-0.135	.495*
	p	0.013	0.006	0.139	0.07	0.001	0.287	0.53	0.014
Tau	*r*	.559**	0.2	0.061	0.124	0.088	.725**	-.439*	0.363
	p	0.005	0.35	0.777	0.563	0.684	0	0.032	0.081
NAA+ NAAG	*r*	-.740**	0.008	0.308	-0.045	-.447*	-.612**	.749**	-.447*
	p	0	0.97	0.143	0.833	0.029	0.001	0	0.029
Glu+Gln	*r*	0.139	-0.084	0.379	-0.098	0.058	.511*	.409*	0.194
	p	0.516	0.696	0.068	0.649	0.789	0.011	0.047	0.364
GPC+ PCho	*r*	.702**	0.397	-0.245	0.354	.612**	0.4	-0.281	.620**
	p	0	0.055	0.248	0.09	0.001	0.053	0.184	0.001
PGC1α	*r*	0.273	-0.143	0.014	0.055	-0.164	-0.027	-0.24	-0.121
	p	0.208	0.514	0.951	0.802	0.455	0.904	0.27	0.581
NRF1	*r*	0.207	-0.104	0.049	0.092	-0.166	-0.082	-0.187	-0.033
	p	0.344	0.636	0.823	0.676	0.45	0.711	0.393	0.88
TFAM	*r*	-.632**	-0.169	0.403	-0.057	-.432*	-.539**	.684**	-0.353
	p	0.001	0.441	0.056	0.798	0.04	0.008	0	0.099

**. Correlation is significant at the 0.01 level (2-tailed).

*. Correlation is significant at the 0.05 level (2-tailed).

(*r*)Pearson Correlation

(*p*)2-Tailed Significance

Table A1 (continued)

		GSH	Ins	Lac	NAA	NAAG	PE	Ser	Tau
pAMPK/AMPK	*r*	-0.268	.559**	-0.054	.414*	-0.229	0.398	-0.334	0.067
	p	0.216	0.006	0.807	0.049	0.292	0.06	0.119	0.76
Cr+PCr	*r*	-0.057	.703**	-0.188	0.391	-.458*	0.169	0.15	0.221
	p	0.793	0	0.38	0.059	0.025	0.429	0.484	0.3
Mac	*r*	-0.265	0.311	-0.021	.438*	-0.045	-0.009	-.636**	-.410*
	p	0.211	0.14	0.922	0.032	0.833	0.965	0.001	0.047
Ala	*r*	0.316	-.448*	0.358	-.530**	0.207	0.212	0.021	0.2
	p	0.133	0.028	0.086	0.008	0.333	0.32	0.924	0.348
Asc	*r*	0.221	.650**	-.458*	0.404	-0.387	-.721**	0.367	-.407*
	p	0.3	0.001	0.024	0.05	0.062	0	0.078	0.048
Asp	*r*	-0.279	.807**	-.486*	.703**	-0.382	0.013	-0.163	-0.193
	p	0.187	0	0.016	0	0.066	0.953	0.445	0.366
bHB	*r*	-0.053	-0.097	0.342	-0.331	0.217	0.333	0.042	0.253
	p	0.806	0.653	0.102	0.114	0.308	0.112	0.846	0.233
GPC	*r*	.449*	.411*	-0.249	0.091	-.407*	-.479*	.607**	0.034
	p	0.028	0.046	0.241	0.672	0.048	0.018	0.002	0.874
PCho	*r*	0.339	-.632**	0.343	-.742**	0.08	0.109	.501*	.559**
	p	0.105	0.001	0.101	0	0.709	0.613	0.013	0.005
Cr	*r*	0.274	0.289	0.15	0.038	-0.138	-0.15	.541**	0.2
	p	0.194	0.171	0.485	0.859	0.52	0.484	0.006	0.35
PCr	*r*	-0.299	.496*	-0.33	0.382	-0.366	0.31	-0.311	0.061
	p	0.156	0.014	0.116	0.066	0.078	0.14	0.139	0.777
GABA	*r*	0.232	0.053	0.056	-0.083	0.175	0.074	0.376	0.124
	p	0.275	0.804	0.796	0.701	0.413	0.73	0.07	0.563
Glc	*r*	.470*	-0.335	-0.099	-.467*	0.133	-0.339	.620**	0.088
	p	0.021	0.109	0.645	0.021	0.536	0.105	0.001	0.684
Gln	*r*	0.364	-.653**	0.34	-.619**	0.089	0.33	0.227	.725**
	p	0.08	0.001	0.104	0.001	0.679	0.115	0.287	0
Glu	*r*	-0.202	.842**	-.522**	.841**	-.490*	-0.326	-0.135	-.439*
	p	0.343	0	0.009	0	0.015	0.12	0.53	0.032
GSH	*r*	1	-0.254	0.117	-0.399	-0.18	-0.232	.495*	0.363
	p		0.232	0.587	0.054	0.399	0.276	0.014	0.081
Ins	*r*	-0.254	1	-.473*	.789**	-0.377	-0.271	-0.071	-.419*
	p	0.232		0.02	0	0.07	0.201	0.743	0.041
Lac	*r*	0.117	-.473*	1	-.528**	0.327	0.369	-0.011	0.368
	p	0.587	0.02		0.008	0.118	0.076	0.96	0.077

		GSH	Ins	Lac	NAA	NAAG	PE	Ser	Tau
NAA	*r*	-0.399	.789**	-.528**	1	-0.2	-0.262	-0.391	-.610**
	p	0.054	0	0.008		0.348	0.216	0.059	0.002
NAAG	*r*	-0.18	-0.377	0.327	-0.2	1	0.14	-0.184	-0.248
	p	0.399	0.07	0.118	0.348		0.514	0.39	0.243
PE	*r*	-0.232	-0.271	0.369	-0.262	0.14	1	-.442*	.559**
	p	0.276	0.201	0.076	0.216	0.514		0.03	0.004
Ser	*r*	.495*	-0.071	-0.011	-0.391	-0.184	-.442*	1	0.276
	p	0.014	0.743	0.96	0.059	0.39	0.03		0.191
Tau	*r*	0.363	-.419*	0.368	-.610**	-0.248	.559**	0.276	1
	p	0.081	0.041	0.077	0.002	0.243	0.004	0.191	
NAA+ NAAG	*r*	-.447*	.722**	-.465*	.976**	0.018	-0.236	-.440*	-.677**
	p	0.029	0	0.022	0	0.932	0.267	0.032	0
Glu+Gln	*r*	0.194	0.156	-0.169	0.193	-.416*	0.025	0.111	0.349
	p	0.364	0.465	0.431	0.366	0.043	0.907	0.605	0.095
GPC+ PCho	*r*	.620**	-0.244	0.113	-.573**	-0.227	-0.256	.875**	.506*
	p	0.001	0.25	0.598	0.003	0.286	0.228	0	0.012
PGC1α	*r*	-0.121	-0.34	0.38	-0.254	0.09	0.247	-0.202	0.093
	p	0.581	0.112	0.074	0.243	0.683	0.257	0.355	0.674
NRF1	*r*	-0.033	-0.252	.418*	-0.238	0.154	0.249	-0.246	0.094
	p	0.88	0.247	0.047	0.275	0.484	0.252	0.258	0.671
TFAM	*r*	-0.353	.670**	-0.253	.690**	-0.169	-0.08	-.519*	-.539**
	p	0.099	0	0.245	0	0.44	0.715	0.011	0.008

**. Correlation is significant at the 0.01 level (2-tailed).

*. Correlation is significant at the 0.05 level (2-tailed).

(*r*)Pearson Correlation

(*p*)2-Tailed Significance

Table A1 (continued)

		NAA+NAAG	Glu+Gln	GPC+PCho	PGC1α	NRF1	TFAM
pAMPK/AMPK	*r*	0.376	0	-0.255	0.061	0.19	.431*
	p	0.077	1	0.241	0.782	0.386	0.04
Cr+PCr	*r*	0.297	0.288	0.094	-0.108	-0.042	0.23
	p	0.159	0.173	0.661	0.623	0.848	0.29
Mac	*r*	.437*	0.033	-.680**	-0.186	-0.111	.544**
	p	0.033	0.877	0	0.396	0.615	0.007
Ala	*r*	-.494*	-0.075	0.162	0.301	0.372	-0.18
	p	0.014	0.729	0.45	0.162	0.08	0.41
Asc	*r*	0.326	-0.037	0.19	-0.145	-0.068	0.297
	p	0.12	0.864	0.373	0.51	0.759	0.169
Asp	*r*	.632**	0.259	-0.282	-0.21	-0.106	.624**
	p	0.001	0.222	0.182	0.336	0.631	0.001
bHB	*r*	-0.289	0	0.179	0.096	0.212	-0.112
	p	0.17	1	0.401	0.662	0.332	0.611
GPC	*r*	0.002	0.043	.541**	-0.362	-0.299	-0.033
	p	0.992	0.844	0.006	0.09	0.166	0.881
PCho	*r*	-.740**	0.139	.702**	0.273	0.207	-.632**
	p	0	0.516	0	0.208	0.344	0.001
Cr	*r*	0.008	-0.084	0.397	-0.143	-0.104	-0.169
	p	0.97	0.696	0.055	0.514	0.636	0.441
PCr	*r*	0.308	0.379	-0.245	0.014	0.049	0.403
	p	0.143	0.068	0.248	0.951	0.823	0.056
GABA	*r*	-0.045	-0.098	0.354	0.055	0.092	-0.057
	p	0.833	0.649	0.09	0.802	0.676	0.798
Glc	*r*	-.447*	0.058	.612**	-0.164	-0.166	-.432*
	p	0.029	0.789	0.001	0.455	0.45	0.04
Gln	*r*	-.612**	.511*	0.4	-0.027	-0.082	-.539**
	p	0.001	0.011	0.053	0.904	0.711	0.008
Glu	*r*	.749**	.409*	-0.281	-0.24	-0.187	.684**
	p	0	0.047	0.184	0.27	0.393	0
GSH	*r*	-.447*	0.194	.620**	-0.121	-0.033	-0.353
	p	0.029	0.364	0.001	0.581	0.88	0.099
Ins	*r*	.722**	0.156	-0.244	-0.34	-0.252	.670**
	p	0	0.465	0.25	0.112	0.247	0
Lac	*r*	-.465*	-0.169	0.113	0.38	.418*	-0.253
	p	0.022	0.431	0.598	0.074	0.047	0.245

		NAA+NAAG	Glu+Gln	GPC+PCho	PGC1α	NRF1	TFAM
NAA	*r*	.976**	0.193	-.573**	-0.254	-0.238	.690**
	p	0	0.366	0.003	0.243	0.275	0
NAAG	*r*	0.018	-.416*	-0.227	0.09	0.154	-0.169
	p	0.932	0.043	0.286	0.683	0.484	0.44
PE	*r*	-0.236	0.025	-0.256	0.247	0.249	-0.08
	p	0.267	0.907	0.228	0.257	0.252	0.715
Ser	*r*	-.440*	0.111	.875**	-0.202	-0.246	-.519*
	p	0.032	0.605	0	0.355	0.258	0.011
Tau	*r*	-.677**	0.349	.506*	0.093	0.094	-.539**
	p	0	0.095	0.012	0.674	0.671	0.008
NAA+ NAAG	*r*	1	0.104	-.636**	-0.241	-0.211	.672**
	p		0.627	0.001	0.268	0.334	0
Glu+Gln	*r*	0.104	1	0.151	-0.29	-0.297	0.111
	p	0.627		0.482	0.179	0.168	0.615
GPC+ PCho	*r*	-.636**	0.151	1	-0.038	-0.048	-.603**
	p	0.001	0.482		0.864	0.827	0.002
PGC1α	*r*	-0.241	-0.29	-0.038	1	.901**	-0.076
	p	0.268	0.179	0.864		0	0.729
NRF1	*r*	-0.211	-0.297	-0.048	.901**	1	0.035
	p	0.334	0.168	0.827	0		0.873
TFAM	*r*	.672**	0.111	-.603**	-0.076	0.035	1
	p	0	0.615	0.002	0.729	0.873	

**. Correlation is significant at the 0.01 level (2-tailed).

*. Correlation is significant at the 0.05 level (2-tailed).

(*r*)Pearson Correlation

(*p*)2-Tailed Significance

Figure A1 – Western Immunoblot of striatum and hippocampus tissue samples.